3812–3821 *Nucleic Acids Research, 2017, Vol. 45, No. 7* *Published online 25 January 2017*
doi: 10.1093/nar/gkx038

Deletion of the *rnl* gene encoding a nick-sealing RNA ligase sensitizes *Deinococcus radiodurans* to ionizing radiation

Brad J. Schmier[1], Xinguo Chen[2], Sandra Wolin[2] and Stewart Shuman[1,*]

[1]Molecular Biology Program, Sloan-Kettering Institute, New York, NY 10065, USA and [2]Cell Biology Department, Yale School of Medicine, New Haven, CT 06536, USA

Received December 20, 2016; Revised January 11, 2017; Editorial Decision January 12, 2017; Accepted January 23, 2017

ABSTRACT

Deinococcus radiodurans **RNA ligase (DraRnl) seals 3′-OH/5′-PO_4 nicks in duplex nucleic acids in which the 3′-OH nick terminus consists of two or more ribonucleotides. DraRnl exemplifies a widely distributed Rnl5 family of nick-sealing RNA ligases, the physiological functions of which are uncharted. Here we show via gene knockout that whereas DraRnl is inessential for growth of** ***D. radiodurans*****, its absence sensitizes the bacterium to killing by ionizing radiation (IR). DraRnl protein is present in exponentially growing and stationary phase cells, but is depleted during the early stages of recovery from 10 kGy of IR and subsequently replenished during the late phase of post-IR genome reassembly. Absence of DraRnl elicts a delay in reconstitution of the 10 kGy IR-shattered** ***D. radiodurans*** **replicons that correlates with the timing of DraRnl replenishment in wild-type cells. Complementation with a catalytically dead mutant highlights that nick sealing activity is important for the radioprotective function of DraRnl. Our findings suggest a scenario in which DraRnl acts at genomic nicks resulting from gap-filling by a ribonucleotide-incorporating repair polymerase.**

INTRODUCTION

Deinococcus radiodurans is a Gram-positive aerobic bacterium with extraordinary tolerance to oxidative stress induced by ionizing radiation (IR), ultraviolet radiation (UV), desiccation and chemical mutagens. The antioxidant defense system of *Deinococcus* ranges from small molecule reactive oxygen species scavengers such as Mn(II) complexes and carotenoids to an extensive enzymatic machinery that includes multiple peroxidases, catalases and superoxide dismutases (1,2).

Despite this impressive free radical defense, a 7 kGy dose of ionizing radiation (IR) generates hundreds of DNA double-strand breaks and thousands of DNA single-strand breaks in exponentially growing cells (2). The 3.28 Mb *Deinococcus* genome comprises two circular chromosomes and two circular plasmids, present in multiple copies per cell during exponential growth. Genome reconstitution after exposure to IR is efficient, faithful and dependent on homologous recombination between overlapping segments of the genome. Genome reassembly occurs in two distinct phases (2–4). In the first phase, termed extended synthesis dependent strand annealing (ESDSA), overlapping genomic fragments are resected in a 5′ to 3′ fashion to generate 3′ single strand DNA tails that are used, via strand invasion promoted by RecA and RadA, to prime new DNA synthesis by DNA polymerases. In the second phase, RecA dependent crossovers convert the long linear DNA repair intermediates into circular genomic replicons. Both ESDSA and RecA-dependent homologous recombination are essential to *D. radiodurans* radiotolerance.

Whereas genome reconstitution is essential to surviving gamma irradiation, oxidative protein damage is also a key factor in IR-induced cell death (1,5). Irreversibly oxidized or misfolded *D. radiodurans* proteins are presumably turned over during post-IR recovery. Consistent with this idea, inactivation of the ATP-dependent ClpPX protease sensitizes *D. radiodurans* to IR and causes a delay in DNA double-strand break repair and cell division (6).

Polynucleotide ligases play an essential role in the execution of DNA replication and repair by joining 3′-OH and 5′-PO_4 termini at DNA nicks to restore the phosphodiester backbone. Ligases accomplish this task via a series of three nucleotidyl transfer steps. In step 1, ligase reacts with either ATP or NAD^+ to form a covalent ligase-(lysyl-Nζ)–AMP intermediate and release pyrophosphate (PP_i) or nicotinamide mononucleotide (NMN). In step 2, AMP is transferred from ligase-adenylate to the 5′-PO_4 DNA end to form a DNA–adenylate intermediate (AppDNA). In step 3, ligase catalyzes attack by a DNA 3′-OH on the DNA–adenylate to seal the two ends via a phosphodiester bond and release AMP. Like all bacteria, *D. radiodurans* has an NAD^+-dependent DNA ligase, LigA (en-

*To whom correspondence should be addressed. Tel: +1 212 639 7145; Email: s-shuman@ski.mskcc.org

coded by gene *DR_2069*). Unlike the prototypal *Escherichia coli* LigA, which is active with magnesium as the cofactor, DraLigA has a distinctive requirement for manganese for its nick-sealing activity (7). A putative second DNA ligase, homologous to the adenylyltransferase catalytic domain of ATP-dependent polynucleotide ligases, is encoded by the *D. radiodurans DR_B0100* gene. The recombinant DR_B0100 protein (named LigB) is capable of reacting with ATP to form a covalent enzyme-AMP adduct (step 1 of the ligase pathway), but attempts to demonstrate an end-joining activity of LigB with either DNA or RNA substrates were unsuccessful (7,8). LigB is encoded by the first ORF in a three-gene operon that includes *DR_B0099*, a poly ADP-ribose glycohydrolase (9), and *DR_B0098*, a 5′-OH polynucleotide kinase (7). This operon is transcriptionally upregulated at 1.5 to 12 h after exposure of *D. radiodurans* to 15 kGy IR (10).

In this study, we query the physiology of the *D. radiodurans* ATP-dependent nick-sealing RNA ligase DraRnl (DR_B0094), which is the founding member of a novel Rnl5 family of ligases found in a variety of bacteria, bacterial viruses, eukarya, and archaea (11–15). DraRnl is a monomeric 342 amino acid protein consisting of C-terminal adenylyltransferase domain fused to a signature N-terminal OB domain that is required for nick joining. DraRnl seals 3′-OH, 5′-PO_4 nicks in duplex RNAs and it requires Mn^{2+} for activity. DraRnl has a strict requirement for RNA at the 3′-OH end of the nick, but is non-selective for DNA versus RNA in the 5′-PO_4 strand or the template strand. Because DraRnl is encoded as the upstream open reading frame of a two-component operon that is transcriptionally upregulated during recovery from ionizing radiation (10), we suspected it might play a role in nucleic acid repair, presumably in a pathway involving nicked duplexes with 3′-OH RNA ends.

Here, we show that DraRnl is present in exponentially growing *D. radiodurans* cells and that its level increases in late stationary phase. DraRnl is depleted within 2 h after 10 kGy IR exposure (conceivably as a consequence of radiation damage to DraRnl itself) and begins to be replenished at 12 h post-IR during the late stages of genome reassembly. We find that deletion of DraRnl renders cells sensitive to gamma radiation and causes a delay in the reconstitution of the IR-shattered genome. Complementation with a ligase-inactive DraRnl-K165M mutant restored the protein level but resulted in IR sensitivity, indicating that nick sealing by DraRnl is relevant to radioresistance. Our results suggest that DraRnl is deployed for ligation at sites of 'ribo-patch' gap repair where ribonucleotides are added to a DNA 3′-OH end by repair polymerases.

MATERIALS AND METHODS

Bacterial growth

Deinococcus radiodurans R1 strains were grown in 1× TGY broth (0.5% tryptone, 0.1% glucose, 0.15% yeast extract) or agar (1.5%) at 30°C. Liquid cultures were incubated on a platform shaker at 250 rpm and growth was measured by monitoring absorbance of the cultures at 600 nm.

Immunodetection of DraRnl in *D. radiodurans* whole cell extracts

Purified tag-free, native DraRnl (11) was used to generate rabbit polyclonal antibodies according to the Pocono Hill Rabbit Farm (Candensis, PA) 91-Day Protocol. Anti-DraRnl was affinity-purified from serum by adsorption to covalently coupled DraRnl using the Pierce Gentle Ag/Ab Binding and Elution Buffer Kit. Purified antibody was dialyzed against phosphate-buffered saline (PBS), aliquoted, and stored at –80°C. For western analysis, cells were resuspended in 10 mM sodium phosphate (pH 7.5), mixed with 4× SDS loading dye, and lysed by heating for 5 min at 95°C. Lysates were spun for 1 min at 14 000 rpm in a microcentrifuge and the supernatants were analyzed by 10% SDS-PAGE. Polypeptides were electrophoretically transferred from the gel to a Hybond Protran Nitrocellulose membrane (GE Healthcare). Membranes were pre-incubated with blocking buffer (20 mM Tris–HCl, pH 7.6, 150 mM NaCl, 0.1% Tween-20, 5% powdered milk). DraRnl was detected using the anti-DraRnl antibody at a dilution of 1:1000 in blocking buffer. The secondary antibody, anti-rabbit IgG–HRP conjugate was obtained from Cell Signaling. GlnA was detected using chicken anti-GlnA primary antibody (Agrisera) at a dilution of 1:5000 and a goat anti-chicken IgY-HRP secondary (Santa Cruz Biotechnology). Both secondary HRP conjugates were incubated with Pierce ECL western blotting substrate for visualization. Where indicated, the DraRnl Westerns were quantified using ImageJ.

Construction of a *D. radiodurans* Δ*rnl* strain

To replace *rnl* with a streptomycin resistance cassette (p*kat-aadA*), three DNA fragments consisting of 1000 bp of DNA upstream of *rnl,* the p*kat-aadA* cassette from pTNK103 (27; a kind gift of J. Battista, Louisiana State University), and 997 bp of DNA downstream of *rnl* were PCR amplified using overlapping primers suitable for Gibson PCR. The three fragments were assembled in a one-pot Gibson PCR reaction (NEB) for 1 h at 50°C. A second Gibson PCR reaction was used to clone the assembled fragments into a BamHI-linearized and antarctic phosphatase-treated pUC19 vector creating pUC-Δ*rnl*. Expression of the streptomycin resistance gene in this cassette is driven by the constitutive promoter of the *D. radiodurans katA* gene (27). $CaCl_2$ competent *D. radiodurans* R1 cells were transformed with pUC-Δ*rnl*, which does not replicate in *D. radiodurans*. Transformants were selected on TGY agar medium containing 5 μg/ml streptomycin. Four rounds of streptomycin selection, cycling between liquid and solid TGY media, were carried out. Each round of liquid selection was performed at escalating doses of streptomycin from 0.5 μg/ml in the first round to 5 μg/ml in the final rounds. Selection on TGY agar was carried out at 5 μg/ml streptomycin. Integration and gene replacement was confirmed by PCR and western analysis.

Construction of Δ95 and Δ*rnl* Δ*95*

To replace either *DR_B0095* (Δ*95*) or both *rnl* and *DR_B0095* (Δ*rnl* Δ*95*) with a hygromycin-resistance cas-

sette (*pkat-hyg*), three DNA fragments consisting of 1046 bp of DNA upstream of *DR_B0095* (Δ*95*) or 901 bp of DNA upstream of *rnl* (Δ*rnl* Δ*95*), the p*kat-hyg* cassette from pTNK104 (27), and 901 bp of DNA downstream of *DR_B0095* were were assembled in parallel one-pot Gibson PCR reactions for 1 h at 50°C. A second Gibson PCR was used to clone the assembled fragments into BamHI-linearized and antarctic phosphatase-treated pUC19 vectors creating pUC-Δ95 and pUC-ΔrnlΔ95. Expression of the hygromycin resistance gene in this cassette is driven by the constitutive promoter of the *D. radiodurans katA* gene. $CaCl_2$ competent *D. radiodurans* R1 cells were transformed with pUC-Δ95 or pUC-ΔrnlΔ95. Transformants were selected on TGY agar supplemented with hygromycin at 37.5 μg/ml. Several rounds of selection, cycling between liquid and solid medium, were carried out with hygromycin concentration at 37.5 μg/ml. Integration and gene replacement was confirmed by PCR and western analysis.

Insertion of the *rnl–DR_B0095* operon into the *amyE locus* of Δ*rnl* Δ*95*

To insert *amyE::rnl-95-kan* into the Δ*rnl* Δ*95* strain, 3516 bp of DNA consisting of the *rnl-DR_B0095* operon fused to a p*kat-kan* kanamycin resistance cassette (27) flanked at the 5′ and 3′ ends by 250 bp of homology to portions of the *amyE* gene (*DR_1472*) was synthesized, sequenced, and inserted into pUC19 by Genscript. The *K165M* allele of the the *rnl* gene was generated by site-directed mutagenesis of *amyE::rnl-95-kan*. $CaCl_2$ competent Δ*rnl* Δ*95* cells were transformed with pUC19-*amyE::rnl-95-kan* or pUC19-*amyE::rnl(K165M)-95-kan*. Transformants were selected on TGY supplemented with 10 μg/ml kanamycin and 37.5 μg/ml hygromycin. After several rounds of antibiotic selection, cycling between liquid and solid media containing 10 μg/ml kanamycin and 37.5 μg/ml hygromycin, the presence of the *amyE*::*rnl-95-kan* insertion was detected by PCR of genomic DNA using primers outside of the *amyE* homology arms. The PCR amplified insert was sequenced to genotype strains as wild-type or *K165M* in the *rnl* gene.

Gamma radiation

Cells were grown to mid-log phase (A_{600} of ∼0.4), washed in 10 mM sodium phosphate (pH 7.5), and then concentrated 100-fold in sodium phosphate buffer prior to gamma irradiation. The concentrated cell suspensions were exposed on ice in 500 μl volumes to a ^{137}Cs gamma ray source (J.L.Shepherd Mark I) at a dose rate of 9.8 Gy/min. Aliquots were removed at the indicated doses, diluted and plated on TGY agar. Survivors were scored by counting colonies after 3–4 days growth at 30°C.

Gamma radiation outgrowth in liquid cultures

Cells irradiated with a 10 kGy dose were diluted in TGY medium to an A_{600} of ∼0.4 and then incubated at 30°C with constant shaking at 250 rpm. Aliquots were withdrawn at various times during the post-irradiation recovery period, centrifuged at 5000g, resuspended in 10 mM sodium phosphate (pH 7.5), and then processed for immunoblotting.

Pulsed field gel electrophoresis

Cells irradiated with a 10 kGy dose were diluted to an A_{600} of ∼0.4 in 1× TGY and grown shaking at 30°C. At various times during the post-irradiation outgrowth, aliquots were removed to prepare DNA plugs as described (17). DNA in the plugs was digested overnight at 37°C with 40 U of the NotI restriction endonuclease. Restriction digested agarose plugs were subjected to pulsed field gel electrophoresis for 22 h at 12°C using the CHEF-DR III electrophoresis system (Bio-Rad). The electrophoresis was carried out at 6 V/cm with a linear pulse of 10–60 s and a switching angle of 120°. Bacteriophage λ cI857-Sam7 DNA concatemers (BioRad) were analyzed in parallel to provide size standards.

RESULTS

DraRnl is constitutively expressed in *D. radiodurans*

Biochemical characterization and structure-function studies of DraRnl were carried out using purified recombinant DraRnl produced in *E. coli* (11–13). However, whether DraRnl is actually present in *D. radiodurans* is unknown. To answer this question, we generated a polyclonal rabbit antibody against recombinant DraRnl. The anti-DraRnl antibody was purified from serum by affinity chromatography to recombinant DraRnl and then used for western blotting to gauge the levels of DraRnl as the bacterial growth cycle progressed, after dilution of an overnight culture into fresh TGY medium, from a logarithmic phase (from 4 to 24 h) into a stationary phase (24–48 h) (Figure 1A).

Immunoblotting of whole cell extracts from equivalent aliquots of cells (as A_{600} units) sampled at 6, 12, 24 and 48 h of growth showed that a ∼37-kDa polypeptide corresponding to DraRnl was present at equivalent levels in exponential phase cells (6 and 12 h) (Figure 1B). Upon entry into stationary phase at 24 h, DraRnl levels increased ∼1.6-fold relative to 6 and 12 h. At 48 h, as stationary phase progressed, there was a further increase in DraRnl levels to ∼2.1-fold greater than in log-phase cells. An antibody against glutamine synthetase (GlnA) was used as a control to gauge equal sample loading.

DraRnl is not required for growth

To examine whether DraRnl is required for growth, we deleted the *rnl* gene by transformation of *D. radiodurans* with a knock-out cassette composed of a *katA* promoter-driven streptomycin-resistance gene (p*katA-aadA*) flanked by genomic DNA segments 5′ and 3′ of the *rnl* ORF (Figure 2A). After multiple rounds of selection for streptomycin resistance, the intended *rnl::aadA* insertion and the absence of an intact *rnl* gene was confirmed by PCR of genomic DNA with diagnostic primers (Figure 2B, left panel). Western analysis with anti-DraRnl antibody verified the absence of DraRnl in the Δ*rnl* strain (Figure 2B, right panel). There was no difference in the growth rates of wild-type and Δ*rnl* strains in TGY medium at 30°C (not shown).

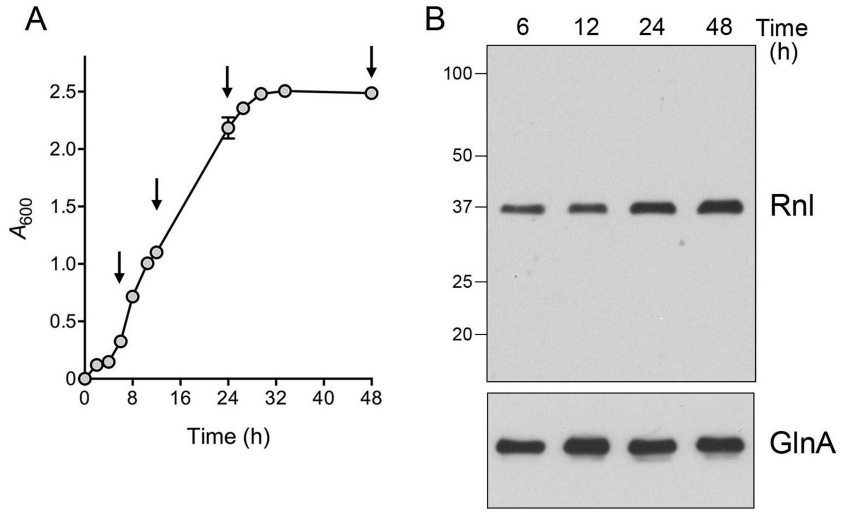

Figure 1. DraRnl is constitutively expressed in *D. radiodurans*. (**A**) Cells were inoculated from an overnight culture into 1× TGY medium to attain A_{600} of 0.05 and the culture was incubated with constant shaking at 30°C. Growth was monitored by plotting A_{600} as a function of time post-inoculation. Aliquots were removed at the times specified by arrows (6, 12, 24 and 48 h). (**B**) Western blotting. Aliquots of cells were normalized to A_{600} of 1.0, pelleted and resuspended in 10 mM sodium phosphate (pH 7.5). Cells were then lysed in SDS loading buffer, resolved by 10% SDS-PAGE, and transferred to a nitrocellulose membrane. An immunoblot with anti-DraRnl antibody is shown in the top panel. The positions and sizes (kDa) of marker polypeptides are indicated on the left. An immunoblot with anti-GlnA antibody is shown in the bottom panel.

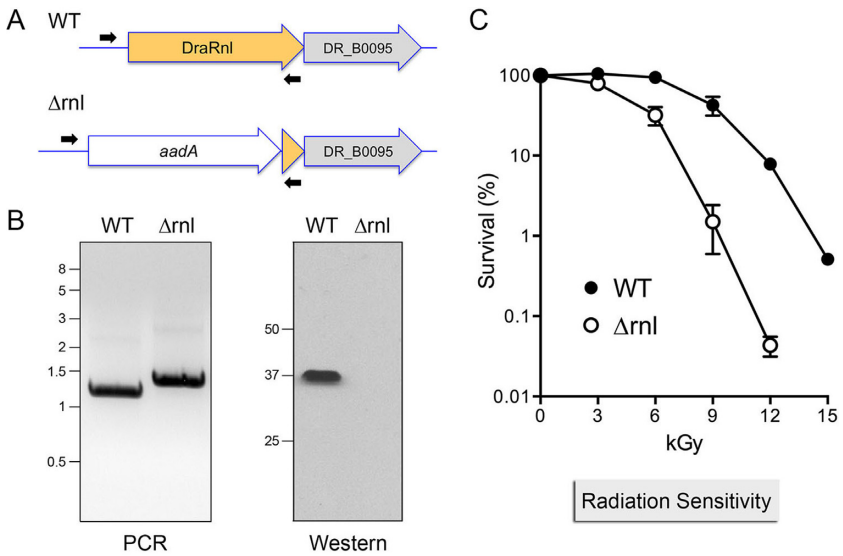

Figure 2. Deletion of *rnl* sensitizes *D. radiodurans* to gamma irradiation. (**A**) Diagram of the *rnl–DR_B0095* locus in wild-type *D. radiodurans* (WT) and after homologous recombination with the *aadA* streptomycin resistance deletion cassette (Δ*rnl*). The co-oriented ORFs encoding DraRnl (in yellow fill) and DR_B0095 (in gray fill) are depicted as horizontal arrows. The *aadA* cassette (white fill) disrupts the *rnl* locus; the Δ*rnl* strain retains 96 bp at the 3′ end of the *rnl* ORF. Positions of the diagnostic PCR primers used for genotyping are shown. (**B**) *Left panel.* PCR confirmation of the Δ*rnl* mutant using the diagnostic primers. The PCR products were analyzed by agarose gel electrophoresis and visualized by staining with ethidium bromide. The positions and sizes (kbp) of linear DNA size markers are indicated on the left. *Right panel*. Western blot of whole cell extracts of equivalent aliquots of exponentially growing WT and Δ*rnl* cells using an anti-DraRnl antibody. The positions and sizes (kDa) of marker polypeptides are indicated on the left. (**C**) WT and Δ*rnl* cells were irradiated on ice in 500 μl volumes using a ^{137}Cs gamma ray source. Aliquots were removed at the indicated doses, diluted, and plated on TGY agar. Survivors were scored by counting colonies after 3–4 days growth at 30°C. Survival (normalized to mock-treated controls for each strain, defined as 100%) is plotted as a function of IR dose. Each datum is the average survival of three separate irradiated cell aliquots ± SEM.

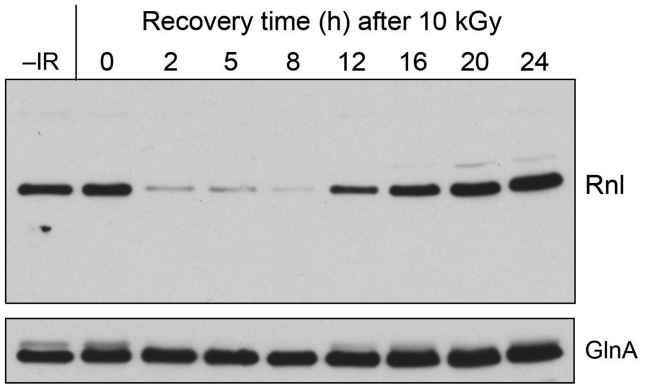

Figure 3. DraRnl is depleted early during recovery from IR and replenished at later stages. Wild-type *D. radiodurans* cells were exposed to a 10 kGy dose of gamma radiation from a ^{137}Cs source, diluted to an A_{600} of 0.4 in TGY medium, and incubated at 30°C with constant shaking. Aliquots were removed at the time specified during post-IR recovery and whole cell extracts were analyzed by SDS-PAGE and immunoblotting with anti-RnlI antibody (*top panel*) and anti-GnlA antibody (*bottom panel*).

Deletion of *rnl* sensitizes *D. radiodurans* to gamma irradiation

The survival of wild-type and Δ*rnl* strains was assessed after exposure to increasing doses of gamma radiation from a ^{137}Cs source. Survival of wild-type *D. radiodurans* was unaffected by 3 and 6 kGy of IR exposure, but declined steadily thereafter as dosage was increased to 9 kGy (43% survival), 12 kGy (7.9% survival) and 15 kGy (0.5% survival).

By contrast, the Δ*rnl* strain was sensitized to all IR doses exceeding 3 kGy, with survival rates of 32% at 6 kGy, 1.5% at 9 kGy and 0.04% at 12 kGy (Figure 2C). Compared to the wild-type strain, Δ*rnl* was 28-fold and 200-fold more sensitive to killing by 9 and 12 kGy of gamma radiation. These results implicate DraRnl as an agent of nucleic acid repair in response to IR damage.

For comparison, we also tested the wild-type and Δ*rnl* strains for their sensitivity to killing by 254 nM UV-C radiation (16). Wild-type *D. radiodurans* was resistant up to a 400 J/m^2 UV-C dose, but died off exponentially as the dose was increased to 600 and 800 J/m^2 (Supplementary Figure S1). The Δ*rnl* strain was 3-fold more sensitive than wild-type to 600 J/m^2 and 5-fold more sensitive to 800 J/m^2 (Supplementary Figure S1). Thus, loss of DraRnl exerts a much greater impact on recovery from gamma radiation than from UV-C.

DraRnl is depleted early during recovery from IR and replenished at later stages

The fate of the DraRnl protein in wild-type *D. radiodurans* cells immediately after exposure to 10 kGy of IR and during post-IR recovery upon re-inoculation into TGY medium was analyzed by Western blotting (Figure 3). The DraRnl level immediately after 10 kGy exposure (time 0) was the same as that in mock-irradiated control cells (–IR). The salient finding was that DraRnl was depleted within 2 h of post-IR recovery and remained depleted at 5 and 8 h. DraRnl reappeared at 12 h and accumulated progressively at 16, 20 and 24 h post-IR (Figure 3). This early depletion

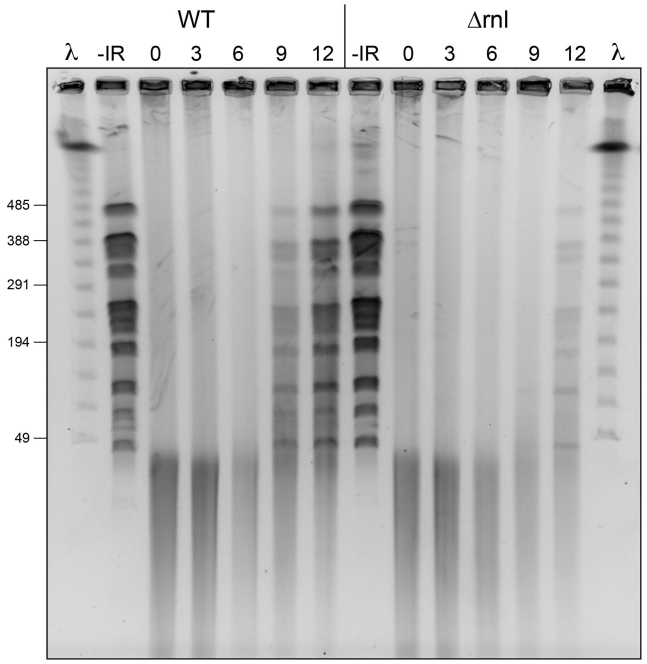

Figure 4. Deletion of *rnl* delays genome reassembly after 10 kGy of gamma irradiation. Wild-type and Δ*rnl* cells exposed to a 10 kGy dose of gamma radiation. Aliquots of cells were removed 0, 3, 6, 9 and 12 h during the post-IR outgrowth and processed for pulsed field gel electrophoresis of NotI-digested cellular DNA as described under Experimental Procedures. Mock-irradiated control cells were analyzed in the lanes labeled –IR. A negative image of the ethidium bromide stained gel is shown. Phage λ DNA concatemers were analyzed in parallel (in lanes λ): the positions and sizes (kb) of selected λ DNAs in the ladder are indicated on the left.

and late restoration of DraRnl was not reflective of generalized protein turnover post-IR, insofar as GlnA levels remained fairly constant during the same period (Figure 3) and Coomassie blue-staining after SDS-PAGE analysis of the protein samples revealed no gross changes in whole-cell polypeptide compositions or levels (not shown). These results suggest DraRnl is turned over early during recovery from gamma irradiation, conceivably because it suffers IR-induced oxidative damage. The replenishment of DraRnl levels in the later stages of recovery has implications for when DraRnl might function in radiation resistance.

Deletion of *rnl* delays genome reassembly after 10 kGy of gamma irradiation

Pulsed-field gel electrophoresis (PFGE) was employed to monitor genome reassembly in wild-type and Δ*rnl* cells after exposure to 10 kGy of gamma radiation. Equivalent aliquots (by A_{600}) of cells immobilized in agarose plugs were digested with NotI endonuclease, which converts the intact *D. radiodurans* genome into large linear DNA fragments (45–476 kb) resolvable by PFGE (2,17). These genomic fragments were evident in the mock-irradiated wild-type and Δ*rnl* samples (Figure 4; –IR). 10 kGy IR exposure shattered the genome, converting the native NotI ladder into a heterogeneous collection of DNA fragments of ≤40 kb (Figure 4; time 0). Genome reassembly, manifest as the restoration of the ladder of discrete NotI fragments,

was evident in wild-type cells at 9 h post-IR, following a 6 h 'early' phase devoted to DNA resection and ESDSA in which the shattered fragments are either unchanged (Figure 4; 3 h) or diminished (Figure 4; 6 h). By 12 h post-IR, wild-type cells had progressed further in genome reconstitution, as gauged by the increased abundance of the intact NotI fragments and the decrement in the smallest shattered fragments.

In the Δ*rnl* strain, the DNA profile during the initial 6 h early phase was identical to that of wild-type cells. The instructive finding was that Δ*rnl* cells suffered a delay of ∼3 h in genome reassembly, to wit: (i) there was scant evidence thereof at 9 h post-IR; and (ii) NotI fragments were assembled in Δ*rnl* cells at 12 h, to a level commensurate with that seen in wild-type cells at 9 h (Figure 4). The timing of the 'late' defect in genome reassembly absent DraRnl correlated with the temporal window during which DraRnl levels are replenished in wild-type cells (Figure 3).

rRNA is not shattered after 10 kGy of gamma irradiation

The substrate specificity of DraRnl, whereby it seals nicks in duplex nucleic acids in which the 3′-OH end is RNA, is compatible in principle with its participation in the repair of radiation-induced DNA damage and/or RNA damage. The experiments presented above implicate DraRnl in restoration of the IR-shattered DNA genome. Yet, the contributions of RNA damage to bacterial sensitivity to IR are uncharted, as are the broken cellular RNAs that might be subject to templated repair by DraRnl. Gamma radiation elicits more single-strand DNA breaks than double strand breaks (2). If single-strand RNA breakage is a factor in IR-induced pathology, or occurs globally as part of a post-IR response to oxidative RNA damage, then we might expect to see a change in the size and/or abundance of 23S and 16S ribosomal RNAs in irradiated *D. radiodurans* cells. To address this issue, RNA isolated from wild-type cells immediately after exposure to 10 kGy of IR and during post-IR recovery after re-inoculation into TGY medium was analyzed by 1.2% formaldehyde-agarose gel electrophoresis. The 23S and 16S rRNA sizes and steady-state levels were unchanged immediately after IR (time 0) and at 1, 2, 5 or 24 h post-IR compared to mock-irradiated controls (Supplementary Figure S2). Note that rRNA is intact at the 2 and 5 h times post-IR when DraRnl is depleted (Figure 3).

Effect of deleting *DR_B0095* and the *rnl–DR_B0095* operon

DraRnl is encoded by the upstream open reading frame of a two-component operon with a gene of unknown function (*DR_B0095*) that encodes a 228-amino acid polypeptide. The N-terminal ∼90–100-aa segment of DR_B0095 displays primary structure similarity to members of the DEDDh family of 3′ exonucleases (18). Because insertional disruption of the upstream *rnl* gene has the potential to exert a polar effect on expression of the downstream *DR_B0095* gene, we generated strains in which either *DR_B0095* or the entire *rnl–DR_B0095* operon was deleted and replaced with a *katA* promoter-driven hygromycin-resistance marker (Figure 5A). The Δ*95* and Δ*rnl* Δ*95* genotypes were confirmed by PCR of genomic DNA with diagnostic primers (Figure 5B). Western analysis showed that the DraRnl protein expression was unaffected in the Δ*95* strain, but effaced in the Δ*rnl* Δ*95* operon knockout (Figure 5C).

Compared to wild-type *D. radiodurans*, deletion of *DR_B0095* elicited modest sensitivity (4-fold) to 9 kGy and 12 kGy of gamma irradiation (Figure 5D), in contrast to the more profound IR sensitivity of the Δ*rnl* strain, signifying that the Δ*rnl* phenotype was not caused merely by a polar effect on *DR_B0095*. The Δ*rnl* Δ*95* operon knockout strain was 3-fold and 6-fold more sensitive to 6 kGy and 9 kGy IR exposure than Δ*rnl* cells (Figure 5D).

DraRnl ligase activity is pertinent to IR survival

Is the nick joining activity of DraRnl needed for its role in protecting *D. radiodurans* from killing by gamma radiation? Or is the Δ*rnl* phenotype caused by the loss of the Rnl protein, e.g. as a structural component of a hypothetical repair protein complex that functions during the late stages of post-IR genome reconstitution? To address this issue, we re-introduced a copy of the *rnl–DR_B0095* operon, marked with a downstream kanamycin-resistance gene, into the inessential *amyE* locus (19) of *D. radiodurans* chromosome I in the Δ*rnl* Δ*95* operon knockout strain (Figure 6A). The *rnl* gene in the operon insert encoded either wild-type DraRnl or a mutated version DraRnl-K165M in which the lysine nucleophile that forms the covalent ligase–AMP intermediate was substituted by methionine (which is isosteric to lysine, minus the ϵ-amino group). Studies of the homologous Rnl5-family enzyme NgrRnl have shown that the Lys-to-Met change abolishes ligase adenylylation and nick joining activity, but does not affect protein structure or the ability of a type-5 Rnl to bind ATP and metal cofactors (15). After several rounds of dual selection for kanamycin resistance (for the *amyE* insertion) and hygromycin resistance (for maintenance of the original Δ*rnl* Δ*95* operon knockout), we confirmed the *amyE::rnl–DR_B0095–kanR* genotypes by diagnostic PCR with primers complementary to *amyE* segments located outside of the insertion cassette (Figure 6A and B). Sequencing of the PCR products verified that the *rnl* loci were either wild-type or *K165M*, as intended. Western analysis showed that Rnl proteins levels were restored in the a*myE::rnl–DR_B0095–kanR* strains with either wild-type or *K165M rnl* alleles (Figure 6C).

Testing the two a*myE::rnl–DR_B0095–kanR* strains for IR survival showed that the *rnl-K165M* allele recapitulated the acute sensitivity of the operon knockout to 9 kGy of gamma radiation (Figure 6D and data not shown). The *amyE*-inserted wild-type *rnl* allele increased survival 13-fold at 9 kGy compared to *rnl-K165M* (Figure 6D), signifying that ligase catalytic activity is important for the protective role of DraRnl against IR. That said, the insertion of the wild-type *rnl–DR_B0095* operon into the *amyE* locus of the Δ*rnl* Δ*95* operon knockout strain did not restore the level of IR resistance of wild-type *D. radiodurans* analyzed in parallel (which was 8-fold more resistant to 9 kGy than the *amyE*-inserted wild-type *rnl* strain; data not shown). It is conceivable that the genomic context surrounding the operon affects expression or function of the operon during post-IR recovery, such that the *amyE* context on the 2.65-Mb chro-

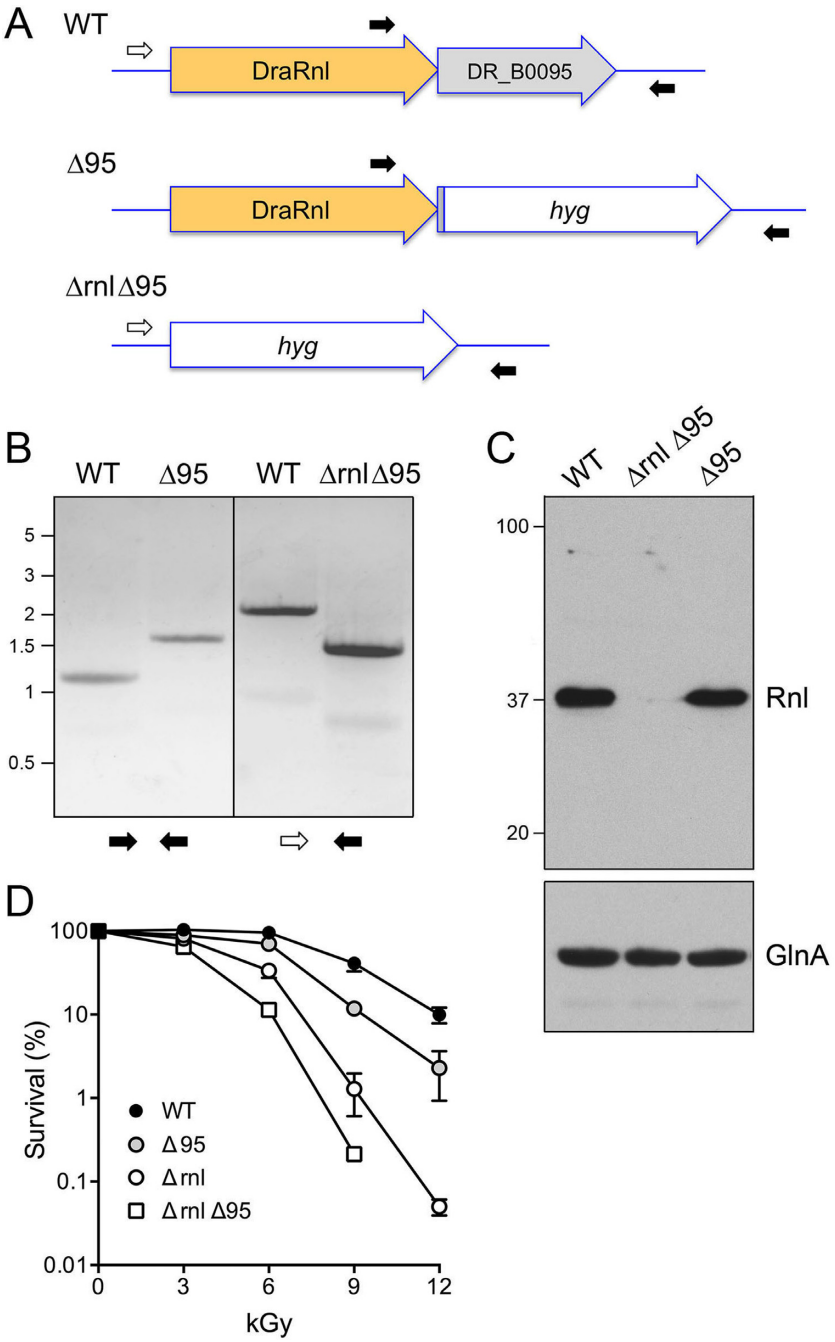

Figure 5. Effect of deleting *DR_B0095* and the *rnl–DR_B0095* operon. (**A**) Diagram of the wild-type *rnl–DR_B0095* operon and after homologous recombination with a hygromycin-resistance cassette (*hyg*) that replaces either *DR_B0095* (Δ95) or the entire operon (Δ*rnl* Δ95). Positions of the diagnostic PCR primers used for genotyping are shown. (**B**) PCR confirmation of the Δ95 and Δ*rnl* Δ95 mutants using the diagnostic primer pairs depicted at bottom. The PCR products were analyzed by agarose gel electrophoresis and visualized by staining with ethidium bromide. The positions and sizes (kb) of linear DNA size markers are indicated on the left. (**C**) Western blot of whole cell extracts of equivalent aliquots of exponentially growing WT, Δ95 and Δ*rnl* Δ95 cells using an anti-DraRnl antibody (*top panel*). The positions and sizes (kDa) of marker polypeptides are indicated on the left. A western blot of the extracts with anti-GlnA is shown in the *bottom panel*. (**D**) WT, Δ95, Δ*rnl* and Δ*rnl* Δ95 cultures were grown as described and then irradiated on ice in 500 μl volumes using a ^{137}Cs gamma ray source. Survival (normalized to mock-treated controls for each strain, defined as 100%) is plotted as a function of IR dose. Each datum is the average survival of three separate irradiated cell aliquots ± SEM.

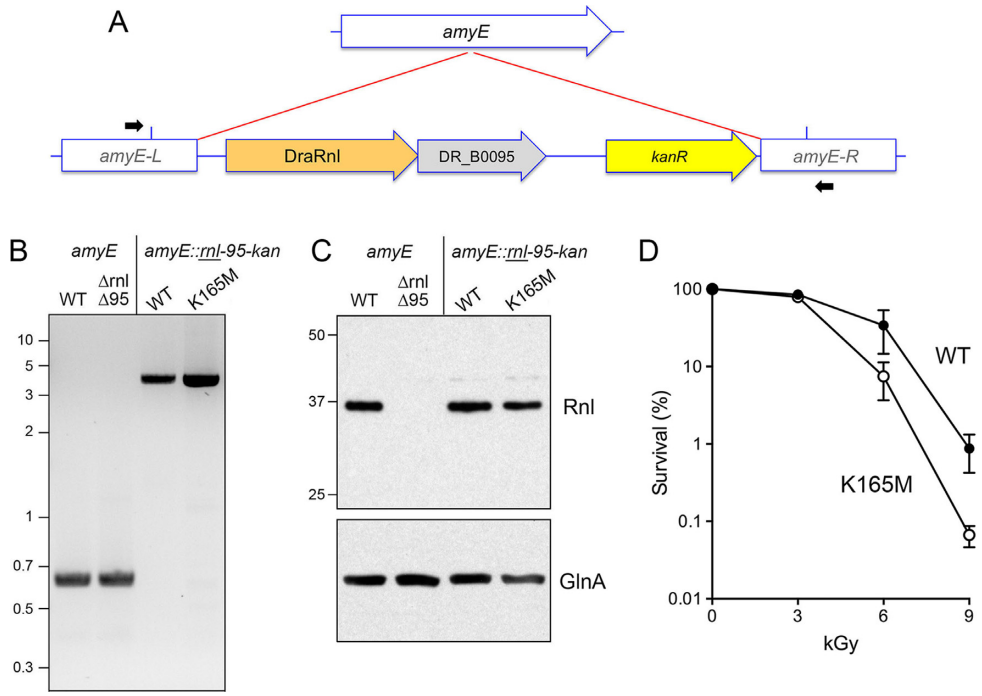

Figure 6. DraRnl ligase activity is pertinent to IR survival. (**A**) Insertion of DraRnl operon into the *amyE* locus. Diagram of the chromosome I *amyE* locus (arrow with white fill) before and after homologous recombination with the *amyE::rnl-95-kan* insertion construct in that disrupts *amyE* and confers kanamycin resistance. The *amyE::rnl-95-kan* insertion was performed in the Δ*rnl* Δ*95* strain. Positions of the diagnostic PCR primers used for genotyping are shown. The primers are located outside the margins (indicated by blue vertical lines) of the *amyE* homology sequences in the *amyE::rnl-95-kan* insertion cassette. (**B**) PCR confirmation of the *amyE::rnl-95-kan* insertions compared to the intact *amyE* locus. The PCR products were analyzed by agarose gel electrophoresis and visualized by staining with ethidium bromide. The positions and sizes (kb) of linear DNA size markers are indicated on the left. (**C**). Western blot of whole cell extracts of equivalent aliquots of the indicated exponentially growing strains using an anti-DraRnl antibody (*top panel*). The positions and sizes (kDa) of marker polypeptides are indicated on the left. A western blot of the extracts with anti-GlnA is shown in the *bottom panel*. (**D**) Δ*rnl* Δ*95* strains with *amyE::rnl-95-kan* inserts encoding wild-type DrRnl or the ligase-dead K165M mutant were irradiated on ice using a ^{137}Cs gamma ray source. Survival (normalized to mock-treated controls for each strain, defined as 100%) is plotted as a function of IR dose. Each datum is the average survival of three separate irradiated cell aliquots ±SEM.

mosome I is less effective than the native operon location on the *D. radiodurans* 178-kbp megaplasmid.

DISCUSSION

Here we provide the first insights to the physiology of DraRnl, the founding member of the Rnl5 clade of ATP-dependent nick-joining RNA ligases. Whereas DraRnl is inessential for growth of *D. radiodurans* under standard laboratory conditions, we show that its absence acutely sensitizes the bacterium to killing by ≥9 kGy gamma radiation, while eliciting only a modest sensitization to UV-C radiation. A unexpected finding was that DraRnl protein is depleted during the early stages of recovery from 10 kGy IR and subsequently replenished during the late phase of post-IR genome reassembly. Absence of DraRnl elicits a delay in the reconstitution of the *D. radiodurans* replicons from repair fragments that correlates with the timing of DraRnl replenishment in wild-type cells. Complementation with a catalytically dead mutant highlights that nick sealing activity is important for the radioprotective function of DraRnl.

Δ*rnl* joins a cadre of IR-sensitive mutants of nucleic acid repair-related genes in *D. radiodurans*. The repair genes can be broadly classified into three groups based on the dose-dependent sensitivity of the mutants to killing by IR compared to wild-type (2). Disruptions of genes such as *recA, recFOR, polA* and *irrE* are the most severe, insofar as they elicit a ≥3 log sensitization at ≤2 kGy of gamma radiation (20–22). The second group of genes includes *drRRA, recG* and *pprA*, deletions of which results in ≥2 log sensitization at 6 kGy (23–25). Δ*rnl* falls into the third category that includes *recN, ddrAB, uvrD, radA, sbcCD* and *polX*, mutations of which sensitize to higher IR dosages (20,26–29). The Δ*uvrD*, Δ*polX* and Δ*sbcCD* mutants (like Δ*rnl*) exhibit a delay in reconstituting the NotI genomic array from IR-shattered fragments (20,28,29).

The nucleic acid substrate specificity of DraRnl suggests a model for its role in repair of IR-induced DNA damage entailing the closure of 3′-OH/5′-PO_4 nicks in the genome in which the 3′-OH nick terminus consists of two or more ribonucleotides (11). Current models of genome recovery post-IR damage call for widespread gap filling after ESDSA and additional gap repair events after homology-dependent replicon assembly from long linear intermediates (2). The polymerase(s) responsible for gap filling are not defined, though PolA and PolX are plausible candidates. We speculate that a *Deinococcus* polymerase is adept at incorporating ribonucleotides during gap filling to generate 3′' ribo-nicks as substrates for sealing by DraRnl. There are several biochemical precedents for bacterial repair polymerases preferentially utilizing rNTPs (30–35) and for DNA repair lig-

ases preferentially sealing nicks with a 3′ ribonucleotide (36). Certain eukaryal PolX-family repair polymerases are also adept at ribonucleotide incorporation (37). *Deinococcus* PolX, mutation of which elicits an IR-sensitivity phenotype similar to that of Δ*rnl*, is reported to have a polymerase activity that adds only two deoxynucleotides to a defined primer-template in a single binding event (38). To our knowledge, there is no published information anent the ability of DraPolX to incorporate ribonucleotides.

Although our results here point to DraRnl as an agent of DNA repair, we cannot exclude the prospect that it has additional roles in RNA repair (either in irradiated cells or under some other stress conditions not interrogated presently), whereby it would seal nicks in dsRNAs or the RNA strand of an RNA:DNA hybrid. The relevance of RNA break repair to post-IR recovery in *D. radiodurans* is speculative at this point, given our findings that rRNA is not shattered by (or during recovery from) a 10 kGy dose of gamma radiation. It is conceivable that dsRNA structures involving *Deinococcus* mRNAs, tRNAs, antisense RNAs (39), or small noncoding RNAs (40) could be subject to breakage and repair, but there is no evidence as yet that such events occur.

The depletion and restoration of DraRnl levels during post-IR recovery is consistent with earlier findings (via 2D-gel analysis of whole-cell extracts and identification of protein spots by N-terminal sequencing) that several *Deinococcus* polypeptides were lost during the initial 2–4 h post-IR interval and then replenished at ≥8 h post-IR (41). DraRnl is a key instance in which a nucleic acid repair enzyme important for IR survival is specifically depleted early and replenished later—at the time when the effect of its genetic ablation of genome reassembly becomes evident. The cause of DraRnl depletion post-IR is not defined, but it is reasonable to think that it directly suffers oxidative damage (e.g. carbonylation) that leads to its accelerated decay by proteolysis.

Finally, the attribution of a DNA repair function to an enzyme identified initially as a nick-sealing RNA ligase has implications for the possible nucleic acid transactions in which other nick-sealing ligases of the Rnl5 and Rnl2 families might participate. Prior to this study, the only nick-sealing RNA ligases that had been assigned biological roles and physiological substrates were the RNA editing ligases (RELs) of the kinetoplastid protozoa *Leishmania* and *Trypanosoma* (42). The RELs, which belong to the Rnl2 family, catalyze the sealing of 3′-OH/5′-PO_4 nicks in duplex RNAs generated during RNA-guided breakage of mRNA precursors and subsequent conversion of the breaks to nicks by either RNA-templated gap filling or resection of single-stranded tails (43,44). Bacteriophage T4 Rnl2 and NgrRnl, which are the structurally well characterized prototypes of Rnl2 and Rnl5 families (15,45), have the same nucleic acid substrate specificity *in vitro* as DraRnl (14,46). It remains to be determined if they are DNA repair enzymes, RNA repair enzymes, or both.

SUPPLEMENTARY DATA

Supplementary Data are available at NAR Online.

ACKNOWLEDGEMENTS

B.S. thanks Dr Weiyi Yang for advice on immunoblotting and the labs of Drs John Petrini and Xiaolan Zhou for advice on PFGE.

FUNDING

National Institutes of Health (NIH) [GM63611 to S.S. and ES022914 to B.S.]. Funding for open access charge: NIH [GM63611].
Conflict of interest statement. None declared.

REFERENCES

1. Daly,M.J. (2009) A new perspective on radiation resistance based on *Deinococcus radiodurans*. *Nat. Rev. Microbiol.*, **7**, 237–245.
2. Slade,D. and Radman,M. (2011) Oxidative stress resistance in *Deinococcus radiodurans*. *Microbiol. Mol. Biol. Rev.*, **75**, 133–191.
3. Zahradka,K., Slade,D., Bailone,A., Sommer,S., Averbeck,D., Petranovic,M., Lindner,A.B. and Radman,M. (2006) Reassembly of shattered chromosomes in *Deinococcus radiodurans*. *Nature*, **443**, 569–573.
4. Slade,D., Lindner,A.B., Paul,G. and Radman,M. (2009) Recombination and replication in DNA repair of heavily irradiated *Deinococcus radiodurans*. *Cell*, **136**, 1044–1055.
5. Radman,M. (2016) Protein damage, radiation sensitivity and aging. *DNA Repair*, **44**, 186–192.
6. Servant,P., Jolivet,E., Bentchikou,E., Mennecier,S., Bailone,A. and Sommer,S. (2007) The ClpPX protease is required for radioresistance and regulates cell division after γ-irradiation in *Deinococcus radiodurans*. *Mol. Microbiol.*, **66**, 1231–1239.
7. Blasius,M., Buob,R., Shevelev,I.V. and Hubscher,U. (2007) Enzymes involved in DNA ligation and end-healing in the radioresistant bacterium *Deinococcus radiodurans*. *BMC Mol. Biol.*, **8**, 69.
8. Kota,S., Kamble,V.A., Rajpurohit,Y.S. and Misra,H.S. (2010) ATP-type DNA ligase requires other proteins for its activity *in vitro* and its operon components for radiation resistance in *Deinococcus radiodurans in vivo*. *Biochem. Cell. Biol.*, **88**, 783–790.
9. Slade,D., Dunstan,M.S., Barkauskaite,E., Weston,R., Lafite,P., Dixon,N., Ahel,M., Leys,D. and Ahel,I. (2011) The structure and catalytic mechanism of a poly(ADP-ribose) glycohydrolase. *Nature*, **477**, 616–620.
10. Liu,Y., Zhou,J., Omelchenko,M.V., Beliaev,A.S., Venkateswaran,A., Stair,J., Wu,L., Thompson,D.K., Xu,D., Rogozin,I.B. *et al.* (2003) Transcriptome dynamics of *Deinococcus radiodurans* recovering from ionizing radiation. *Proc. Natl. Acad. Sci. U.S.A.*, **100**, 4191–4196.
11. Martins,A. and Shuman,S. (2004) An RNA ligase from *Deinococcus radiodurans*. *J. Biol. Chem.*, **279**, 50654–50661.
12. Raymond,A. and Shuman,S. (2007) *Deinococcus radiodurans* RNA ligase exemplifies a novel ligase clade with a distinctive N-terminal module that is important for 5′-PO_4 nick sealing and ligase adenylylation but dispensable for phosphodiester formation at an adenylylated nick. *Nucleic Acids Res.*, **35**, 839–849.
13. Schmier,B.J. and Shuman,S. (2014) Effects of 3′-OH and 5′-PO_4 base mispairs and damaged base lesions on the fidelity of nick sealing by *Deinococcus radiodurans* RNA ligase. *J. Bacteriol.*, **196**, 1704–1712.
14. Unciuleac,M.C. and Shuman,S. (2015) Characterization of a novel eukaryal nick-sealing RNA ligase from *Naegleria gruberi*. *RNA*, **21**, 824–832.
15. Unciuleac,M.C., Goldgur,Y. and Shuman,S. (2015) Structure and two-metal mechanism of a eukaryal nick-sealing RNA ligase. *Proc. Natl. Acad. Sci. U.S.A.*, **112**, 13868–13873.
16. Chen,X., Quinn,A.M. and Wolin,S.L. (2000) Ro ribonucleoproteins contribute to the resistance of *Deinococcus radiodurans* to ultraviolet irradiation. *Genes Dev.*, **14**, 777–782.
17. Harris,D.R., Tanaka,M., Saveliev,S.V., Jolivet,E., Earl,A.M., Cox,M.M. and Battista,J.R. (2004) Preserving genome integrity: the DdrA protein of *Deinococcus radiodurans* R1. *PLoS Biol.*, **2**, e304.
18. Cheng,Y. and Patel,D.J. (2004) Crystallographic structure of the nuclease domain of 3′hExo, a DEDDh family member, bound to rAMP. *J. Mol. Biol.*, **343**, 305–312.

19. Meima,R., Rothfuss,H.M., Gewin,L. and Lidstrom,M.E. (2001) Promoter cloning in the radioresistant bacterium *Deinococcus radiodurans*. *J. Bacteriol.* **183**, 3169–3175.
20. Bentchikou,E., Servant,P., Coste,G. and Sommer,S. (2010) A major role of the RecFOR pathway in DNA double-strand-break repair through ESDSA in *Deinococcus radiodurans*. *PLoS Genet.*, **6**, e10000774.
21. Earl,A.M., Mohundro,M.M., Mian,I.S. and Battista,J.R. (2002) The IrrE protein of *Deinococcus radiodurans* R1 is a novel regulator of *recA* expression. *J. Bacteriol.*, **184**, 6216–6224.
22. Gutman,P.D., Fuchs,P.I., Ouyang,L.I. and Minton,K.W. (1993) Identification, sequencing, and targeted mutagenesis of a DNA polymerase gene required for the extreme radioresistance of *Deinococcus radiodurans*. *J. Bacteriol.*, **175**, 3581–3590.
23. Wang,L., Xu,G., Chen,H., Zhao,Y., Xu,N., Tian,B. and Hua,Y. (2008) DrRRA: a novel response regulator essential for the extreme radioresistance of *Deinococcus radiodurans*. *Mol. Microbiol.*, **67**, 1211–1222.
24. Wu,Y., Chen,W., Zhao,Y., Xu,H. and Hua,Y. (2009) Involvement of RecG in H_2O_2-induced damage repair in *Deinococcus radiodurans*. *Can. J. Microbiol.* **55**, 841–848.
25. Narumi,I., Satoh,K., Cui,S., Funayama,T., Kitayama,S. and Watanabe,H. (2004) PprA: a novel protein from *Deinococcus radiodurans* that stimulates DNA ligation. *Mol. Microbiol.*, **54**, 278–285.
26. Funayama,T., Narumi,I., Kikuchi,M., Kitayama,S., Watanabe,H. and Yamamoto,K. (1999) Identification and disruption analysis of the *recN* gene in the extremely radioresistant bacterium *Deinococcus radiodurans*. *Mutat. Res.*, **435**, 151–161.
27. Tanaka,M., Earl,A.M., Howell,H.A., Park,M.J., Eisen,J.A., Peterson,S.N. and Battista,J.R. (2004) Analysis of *Deinococcus radiodurans's* transcriptional response to ionizing radiation and desiccation reveals novel proteins that contribute to extreme radioresistance. *Genetics*, **168**, 21–33.
28. Lecointe,F., Shevelev,I.V., Bailone,A., Sommer,S. and Hübscher,U. (2004) Involvement of an X family DNA polymerase in double-strand break repair in the radioresistant organism *Deinococcus radiodurans*. *Mol. Microbiol.*, **53**, 1721–1730.
29. Bentchikou,E., Servant,P., Coste,G. and Sommer,S. (2007) Additive effects of SbcCD and PolX deficiencies in the in vivo repair of DNA double-strand-breaks in *Deinococcus radiodurans*. *J. Bacteriol.*, **198**, 4784–4790.
30. Zhu,H. and Shuman,S. (2005) Novel 3′-ribonuclease and 3′-phosphatase activities of the bacterial non-homologous end-joining protein, DNA ligase D. *J. Biol. Chem.*, **280**, 25973–25981.
31. Zhu,H., Nandakumar,J., Aniukwu,J., Wang,L.K., Glickman,M.S., Lima,C.D. and Shuman,S. (2006) Atomic structure and NHEJ function of the polymerase component of bacterial DNA ligase D. *Proc. Natl. Acad. Sci. U.S.A.*, **103**, 1711–1716.
32. Zhu,H., Bhattarai,H., Yan,H., Shuman,S. and Glickman,M. (2012) Characterization of *Mycobacterium smegmatis* PolD2 and PolD1 as RNA/DNA polymerases homologous to the POL domain of bacterial DNA ligase D. *Biochemistry.*, **51**, 10147–10158.
33. Pitcher,R.S., Brissett,N.C., Picher,A.J., Andrade,P., Juarez,R., Thompson,D., Fox,G.C., Blanco,L. and Doherty,A.J. (2007) Structure and function of a mycobacterial NHEJ DNA repair polymerase. *J. Mol. Biol.*, **366**, 391–405.
34. Ordonez,H., Uson,M.L. and Shuman,S. (2014) Characterization of three *Mycobacterial* DinB (DNA polymerase IV) paralogs highlights DinB2 as naturally adept at ribonucleotide incorporation. *Nucleic Acids Res.*, **42**, 11056–11070.
35. Ordonez,H. and Shuman,S. (2014) *Mycobacterium smegmatis* DinB2 misincorporates deoxyribonucleotides and ribonucleotides during templated synthesis and lesion bypass. *Nucleic Acids Res.*, **42**, 12722–12734.
36. Zhu,H. and Shuman,S. (2008) Bacterial nonhomologous end joining ligases preferentially seal breaks with a 3′-OH monoribonucleotide. *J. Biol. Chem.*, **283**, 8331–8339.
37. Nick-McElhinny,S.A. and Ramsden,D.A. (2003) Polymerase mu is a DNA-directed DNA/RNA polymerase. *Mol. Cell. Biol.*, **23**, 2309–2315.
38. Khairnar,N.P. and Misra,H.S. (2009) DNA polymerase X from *Deinococcus radiodurans* implicated in bacterial tolerance to DNA damage is characterized as a short patch base excision repair polymerase. *Microbiology*, **155**, 3005–3014.
39. Luan,H., Meng,N., Fu,J., Chen,X., Xu,X., Feng,Q., Jiang,H., Dai,J., Yuan,X., Lu,Y. and Roberts,A.A. (2014) Genome-wide transcriptome and antioxidant analyses on gamma-irradiated phases of *Deinococcus radiodurans* R1. *PLoS One*, **9**, e85649.
40. Tsai,C.H., Liao,R., Chou,B. and Contreras,L.M. (2015) Transcriptional analysis of *Deinococcus radiodurans* reveals novel small RNAs that are differentially expressed under ionizing radiation. *Appl. Environ. Microbiol.*, **81**, 1754–1764.
41. Joshi,B., Schmid,R., Altendorf,K. and Apte,S.K. (2004) Protein recycling is a major component of post-irradiation recovery in *Deinococcus radiodurans* strain R1. *Biochem. Biophys. Res. Commun.*, **320**, 1112–1117.
42. Schnaufer,A., Panigrahi,A.K., Panicucci,B., Igo,R.P., Salavati,R. and Stuart,K. (2001) An RNA ligase essential for RNA editing and survival of the bloodstream form of *Trypanosoma brucei*. *Science*, **291**, 2159–2162.
43. Blanc,V., Alfonzo,J.D., Aphasizhev,R. and Simpson,L. (1999) The mitochondrial RNA ligase from *Leishmania tarentolae* can join RNA molecules bridged by a complementary RNA. *J. Biol. Chem.*, **274**, 24289–24296.
44. Palazzo,S.S., Panigrahi,A.K., Igo,R.P., Salavati,R. and Stuart,K. (2003) Kinetoplastid RNA editing ligases: Complex association, characterization, and substrate requirements. *Mol. Biochem. Parasitol.* **127**, 161–167.
45. Nandakumar,J., Shuman,S. and Lima,C.D. (2006) RNA ligase structures reveal the basis for RNA specificity and conformational changes that drive ligation forward. *Cell*, **127**, 71–84.
46. Nandakumar,J. and Shuman,S. (2004) How an RNA ligase discriminates RNA damage versus DNA damage. *Mol. Cell.*, **16**, 211–221.